JOURNAL OF GUIDANCE, CONTROL, AND DYNAMICS
Vol. 25, No. 2, March–April 2002

Experiments on Command Shaping Control of a Manipulator with Flexible Links

Marcello Romano
Politecnico di Milano, 20158 Milan, Italy
Brij N. Agrawal
Naval Postgraduate School, Monterey, California 93943
and
Franco Bernelli-Zazzera
Politecnico di Milano, 20158 Milan, Italy

Minimizing vibrations of a maneuvered flexible manipulator is a challenging task. Results are presented of a series of experimental tests carried out on the Space Robot Simulator assembly, which has been set up at the Spacecraft Research and Design Center of the Naval Postgraduate School. The manipulator is planar with two rotational degrees of freedom and two links, of which either one or both can be flexible in bending. The manipulator floats on air cushions on a granite table. The task of the experiments was to test the effectiveness of the command input shaping technique on the near-minimum-time tracking control of a flexible manipulator. A recently introduced sliding mode control method with smooth joint friction compensation was applied to track either an open- or a closed-reference end-effector path, mapped into joint space. This controller guarantees a very precise tracking of the joint reference motion, despite the high and poorly modeled joint friction torques. Satisfying results, in terms of vibration reduction, have been obtained on point-to-point trajectories and on closed-path trajectories. The results are compared with those obtained with a different command shaping technique.

Marcello Romano is currently a postdoctoral researcher at Dipartimento di Ingegneria Aerospaziale of Politecnico di Milano. He has been awarded a U.S. National Research Council one-year research associateship, to begin in August 2001 at the Spacecraft Research and Design Center of the Naval Postgraduate School. He received his Ph.D. in Aerospace Engineering in 2001 and his Laurea Degree in Aerospace Engineering in 1997, both from Politecnico di Milano. His main research interests are the control of space robots, the attitude control of satellites, and the on ground experimenting of these systems. He is an AIAA Member.

Brij N. Agrawal is a professor in the Department of Aeronautics and Astronautics and Director of the Spacecraft Research and Design Center. He came to the Naval Postgraduate School in 1989 and since then has initiated a new M.S. curriculum in astronautical engineering in addition to establishing the Spacecraft Research and Design Center. He also has developed research programs in attitude control of flexible spacecraft, smart structures, and space robotics. He received his Ph.D. in Mechanical Engineering from Syracuse University in 1970 and his M.S. in Mechanical Engineering from McMaster University in 1968. He is an AIAA Associate Fellow.

Franco Bernelli-Zazzera received his Laurea Degree in Aeronautical Engineering in the academic year 1984/85, with full marks, and in 1990 he received his Ph.D. in Aerospace Engineering, both from Politecnico di Milano. In November 1992, he became Associate Professor and, in March 2001, Full Professor at Politecnico di Milano, where he currently teaches and performs research in the fields of space flight mechanics and aerospace control systems. He is an AIAA Senior Member.

Received 16 February 2001; revision received 2 July 2001; accepted for publication 19 July 2001.

I. Introduction

VIBRATION reduction is a critical problem related to the maneuvering of space robots, which are light, slender, and flexible. Command shaping techniques are possible solutions to that problem.

A set of command shaping techniques exists. These techniques work by altering the shape of either the actuator commands, or the reference outputs, to reduce the oscillation of the system response. Input shaping refers to a particular command shaping technique that exploits the convolution of the reference signal with a sequence of impulses to reduce the system vibrations. Smith[1] first proposed that idea in his work on Posicast control. Singer and Seering[2] improved Smith's[1] original idea by increasing the robustness. They[2] obtained promising simulation results of input shaping control of the space shuttle remote manipulator system. Singhose et al.[3] studied an input shaping controller for slewing a flexible spacecraft. Banerjee and Singhose[4,5] proposed the application of input shaping for the minimum-time control of a two-link flexible manipulator. Song et al.[6] treated the application of input shaping for reduction of vibration of a flexible spacecraft, using pulse-width pulse-frequency-modulated thrusters. Another command shaping approach, whose principle is to smooth the bang–bang input with a spline approximation of the sign function, was proposed by Junkins et al.[7] and studied by Hecht and Junkins to deal with the problem of near-minimum-time control of a flexible manipulator.[8] Mimmi et al. studied a different command shaping technique derived by the design of cam profiles.[9] All of the referred papers prove the effectiveness of command shaping using numerical simulations. There are also several papers reporting experimental verifications of those techniques. In Ref. 10, the results are discussed of application of input shaping on the MACE experiment, which flew on the space shuttle in 1995. In Ref. 11, the results are reported of applying the input shaping control on a *XY* stage machine carrying a flexible beam. In Refs. 12–14, the experimental testing of command shaping techniques on flexible link manipulators is reported.

A second critical problem, which often affects space manipulators, in addition to structural flexibility, is the stick–slip friction at the joints. In fact, space manipulators are usually actuated by motors with gears. Numerous methods are proposed in the literature to cope with the problem of friction in mechanisms (see Armstrong et al.[15] for a survey). In particular, Song[16] introduces a promising sliding-mode tracking control method, exploiting a smooth friction compensation action.

To carry out the experiments reported in this paper, a testbed, called the Space Robot Simulator, was purposely designed and setup at the Spacecraft Research and Design Center of the Naval Postgraduate School. This is a planar manipulator with two rotational degrees of freedom and two links, either one of which can be flexible as regards bending in the plane of motion. The manipulator floats on air cushions on a granite table.

Our new contributions, obtained by using the Space Robot Simulator and described in this paper, are as follows.

1) A detailed experimental verification is provided of the input shaping method for the tracking control of a manipulator with highly flexible links. In particular, the challenging case of near-minimum-time reference motion has been considered.

2) The input shaping technique is compared with the smoothed bang–bang command shaping technique proposed in Ref. 7.

3) The sliding-mode tracking controller with smooth friction compensation proposed in Ref. 16 is experimentally verified.

Section II is an introduction to the two command shaping methods. Section III describes the sliding-mode tracking controller. The experimental setup is described in Sec. IV. Finally, the results of the experiments are reported in Sec. V.

II. Command Shaping Methods

A. Input Shaping

The input shaping method, in principle, works by creating a command signal that cancels the vibration produced on the system to which it is applied. The method adopted for the present research is based on linear system theory.

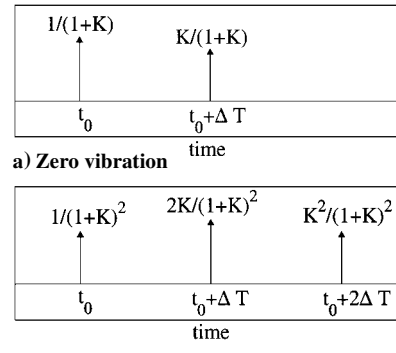

Fig. 1 Impulse sequences.

Suppose we have an underdamped second-order linear system. Its response to an impulsive input at time t_0 is a decaying sinusoid. If, after the application of a first impulse to the system, a second impulse, with suitable relative amplitude and phase with respect to the first, is applied, the vibration due to the first impulse is completely eliminated by the second input. The relative amplitude and phase of the two impulses satisfying this property, calculated considering the superposition of the responses to the single impulses and applying the constraints of zero residual vibration (ZV) is shown in Fig. 1a.

The pulse train parameters are given by

$$K = \exp\left(-\zeta\pi \Big/ \sqrt{1-\zeta^2}\right) \qquad \Delta T = \pi \Big/ \omega_0 \sqrt{1-\zeta^2} \tag{1}$$

where ζ is the damping ratio of the plant and ω_0 is its undamped natural frequency.

The method just described was the main idea of Smith's Posicast control.[1] Singer and Seering[2] show that with a train of two impulses the robustness against uncertainty in the modal frequency ω_0 is weak. To enhance the robustness, they propose to use a train of three impulses, instead of two, and they calculate the relative amplitudes and phases of those impulses, imposing a zero vibration derivative condition (ZVD) beside the ZV condition. That is, the derivative of the constraints with respect to ω_0 is set equal to zero. The resulting three-impulse train is shown in Fig. 1b. The ZVD impulse train provides robustness increased to $\pm 20\%$ of frequency variations. The same expressions that guarantee zero derivatives of the constraints with respect to frequency also guarantee zero derivatives with respect to damping ratio. High variations in damping ratio are tolerated. The process of adding robustness could be further extended, including second derivative of the zero residual vibration constraints and calculating the parameters of a four-impulses train.

The described impulse sequences can be convolved to an arbitrary input, to obtain the same vibration-reducing properties of the impulsive input case. The sequence, therefore, becomes a prefilter, called an input shaper, for any input to be given to the system. There is a time penalty, resulting from the input shaper prefiltering, equal to the length of the impulse sequence. The input shaper impulse sequences can be generalized to consider more than one vibration mode, convolving each of the impulse trains designed for specific modes.

Even though no general statement can be made a priori regarding the applicability of input shaping to nonlinear systems, the effectiveness of input shaping to control various specific nonlinear systems has been proved by numerical simulation. In particular, the case of a two-links manipulator with flexible links is treated in Ref. 5.

B. Command Smoothing

In addition to input shaping, a second command shaping method has been considered for the experiments performed. This technique will be called hereafter smoothed bang–bang command.

To avoid the instantaneous switches of the near-minimum-time bang–bang law, which, applied to flexible systems, excite the poorly modeled higher modes, Junkins et al.[7] proposed to use a continuous spline approximation of the sign function. It is here recalled that the bang–bang command gives the minimum-time control only in

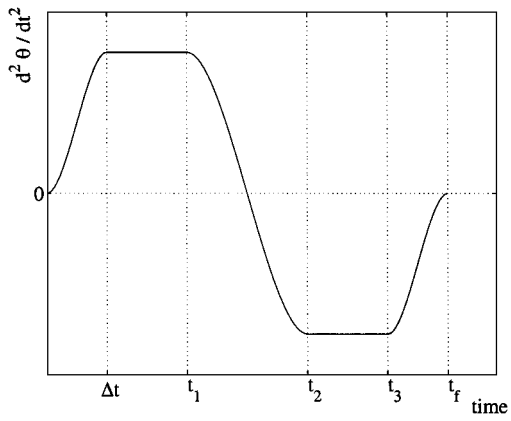

Fig. 2 Smoothed bang–bang command profile.

case of a rigid-body, single-axis control problem. For the manipulator maneuvering, better time minimum control solutions can be obtained by the technique proposed in Ref. 17 and used in Ref. 18. Nevertheless, the bang–bang command is used here for the sake of simplicity to test the effectiveness of the investigated control methods.

The near-minimum-time, smoothed bang–bang reference command, for a single-axis rest-to-rest motion, has the following form (Fig. 2):

$$\ddot{\theta}_{\text{ref}} = \text{sign}(\theta_f - \theta_0)\ddot{\theta}_{\max} f(\Delta t, t_f, t) \tag{2}$$

where $\ddot{\theta}_{\max} = u_{\max}/I$ is the maximum angular acceleration, which is a function of the saturation torque $u_{\max}$ and of I, the inertia of the undeformed system; t_f is the maneuver time; $\Delta t = \alpha t_f$ is the rise time, which is a function of the smoothing parameter $0 < \alpha < 0.25$; and $f(\Delta t, t_f, t)$ is the smooth sign function approximation, given by

$$\begin{aligned}
&(t/\Delta t)^2[3 - 2(t/\Delta t)] && 0 \le t \le \Delta t \\
&1 && \Delta t \le t \le t_1 \\
&1 - 2[(t - t_1)/2\Delta t]^2\{3 - 2[(t - t_1)/2\Delta t]\} && t_1 \le t \le t_2 \\
&-1 && t_2 \le t \le t_3 \\
&-1 + [(t - t_3)/\Delta t]^2\{3 - 2[(t - t_3)/\Delta t]\} && t_3 \le t \le t_f
\end{aligned} \tag{3}$$

where $t_1 = (t_f/2 - \Delta t)$, $t_2 = (t_f/2 + \Delta t)$, and $t_3 = (t_f - \Delta t)$.

When Eq. (2) is integrated, considering Eq. (3), the following relationship between maneuver time, boundary conditions, maximum angular acceleration, and smoothing parameter is obtained:

$$t_f^2 = \frac{(\theta_f - \theta_0)}{\ddot{\theta}_{\max}\left(\frac{1}{4} - \frac{1}{2}\alpha + \frac{1}{10}\alpha^2\right)} \tag{4}$$

and $\dot{\theta}_{\text{ref}}(t)$ and $\theta_{\text{ref}}(t)$ are obtained by integration of Eq. (2), once the values of the parameters are fixed. In particular, for $\alpha = 0$ the bang–bang reference command is obtained.

III. Sliding-Mode Tracking Control

Command shaping is usually applied as an open-loop technique to reduce vibrations because it does not require a measurement of the state of the system, but it can also be applied to the reference signals of a closed-loop system. In this last way, it has been applied in the present research. In fact, in our case, the two command shaping techniques, described in the preceding section, have been applied to the reference acceleration of the manipulator, either angular acceleration or acceleration along the path. Then, a closed-loop tracking control method has been applied, at the joints level, to follow those reference accelerations.

In particular, a sliding-mode tracking control method with friction compensation, which was recently proposed in Ref. 16, has been for the first time applied in our experiments to counteract the high and varying static friction torques. A good tracking of the joints motion was needed to reach our main goal of verifying the effectiveness of input shaping for vibrations reduction.

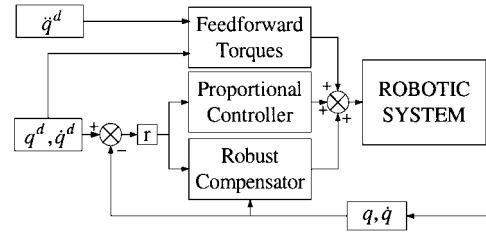

Fig. 3 Block diagram of controller.

A brief description of the sliding mode tracking control follows.[16] The vectorial dynamic equation of a n-degree-of-freedom (DOF) manipulator, assumed to be rigid, has the form

$$M(\boldsymbol{q})\ddot{\boldsymbol{q}} + C(\boldsymbol{q}, \dot{\boldsymbol{q}})\dot{\boldsymbol{q}} + \boldsymbol{g}(\boldsymbol{q}) = \boldsymbol{\Gamma}_{\text{appl}} + \boldsymbol{\Gamma}_{\text{fric}} \tag{5}$$

where $\boldsymbol{q} \in \mathbb{R}^n$ is the vector of joint displacements, $M \in \mathbb{R}^{n \times n}$ is the inertia matrix, $C \in \mathbb{R}^{n \times n}$ accounts for the Coriolis and centrifugal forces, $\boldsymbol{g} \in \mathbb{R}^n$ is the vector of gravity torques, $\boldsymbol{\Gamma}_{\text{appl}} \in \mathbb{R}^n$ is the vector of the applied torques, and $\boldsymbol{\Gamma}_{\text{fric}} \in \mathbb{R}^n$ is the vector of joint friction torques. The friction can be generally described as a composition of two different processes: the static process, also called stick or coulomb friction, when the objects in contact are stationary, and the dynamic process, also called slip friction, when sliding motion is involved. Many different friction models exist.[15] To derive the controller used, the stick friction is considered characterized only by the maximum static torque, below which the state remains static, and the slip friction is upper bounded with a viscous term.

During the controller design, the robot geometric parameters are considered uncertain, and the joints friction model unknown. Nevertheless, the two following assumptions are made. 1) The upper bound of each uncertain system parameter is known. 2) The upper bound of the maximum static friction torque and upper bounding function of the viscous friction torque at each joint are known.

Some definitions are needed to express the robust controller. Let $\hat{M}$, $\hat{C}$, and $\hat{\boldsymbol{g}}$ denote the nominal versions of the actual terms M, C, and $\boldsymbol{g}$. The corresponding uncertainty residues are $\tilde{M}$, $\tilde{C}$, and $\tilde{\boldsymbol{g}}$. The position and velocity errors are $\boldsymbol{e} = \boldsymbol{q} - \boldsymbol{q}_d$ and $\dot{\boldsymbol{e}} = \dot{\boldsymbol{q}} - \dot{\boldsymbol{q}}_d$. The variable, which set equal to zero defines the sliding surface, is defined as $\boldsymbol{r} = \dot{\boldsymbol{e}} + \Lambda \boldsymbol{e}$, where Λ is a constant positive diagonal matrix.

The considered robust controller, whose block diagram is shown in Fig. 3, is given by

$$\boldsymbol{\Gamma}_{\text{appl}} = \boldsymbol{\Gamma}_{\text{ff}} - K\boldsymbol{r} - \varrho_0 \tanh[(a + bt)\boldsymbol{r}] \tag{6}$$

and consists of three parts: 1) a feedforward term, $\boldsymbol{\Gamma}_{\text{ff}}$, computed on the basis of the nominal system model, that is considering the robot rigid, having Eq. (5), and no friction; 2) a linear feedback, $-K\boldsymbol{r}$, where K is a positive diagonal gain matrix; and 3) a robust control term, $-\varrho_0 \tanh[(a + bt)\boldsymbol{r}]$, designed to compensate the stick–slip friction. The nonlinear compensator can exert torques to drive the robot along the desired trajectory, when the proportional feedback is too weak to overcome the friction torque. Here a and b are positive gains, and $\varrho_0 = \varrho_0(\boldsymbol{q}, \boldsymbol{q}_d, \dot{\boldsymbol{q}}, \dot{\boldsymbol{q}}_d)$ is a positive scalar function wrapping the uncertainty. The factor depending on the hyperbolic tangent makes a smooth contribution to the control action, which aims to maintain the sliding condition $r = 0$, then tracks the desired joints trajectory, compensating the friction action. In particular it is $\varrho_0 = k_1\|\tilde{M}\|\|\dot{\boldsymbol{v}}\| + k_2\|\tilde{C}\|\|\boldsymbol{v}\| + k_3\|\tilde{\boldsymbol{G}}\| + \xi(\boldsymbol{q}, \dot{\boldsymbol{q}})$, where k are gains greater than 1, $\xi = f_s + f_d\|\dot{\boldsymbol{q}}\|$ are upper bounds of the friction, and f_s and f_d are positive constants. Moreover, $\boldsymbol{v} = \dot{\boldsymbol{q}}_d - \Lambda \boldsymbol{e}$.

Global asymptotic stability of this closed-loop controller is proved in Ref. 16, exploiting Lyapunov's direct method.

IV. Space Robot Simulator Testbed

This section reports a description of the elements of the Space Robot Simulator (SRS) testbed, which was designed and set up at the Spacecraft Research and Design Center of the Naval Postgraduate School. A schematic diagram of the testbed is shown in Fig. 4.

Table 1 Geometric data of the SRS manipulator in two configurations: RF and FF

Area	Mass, kg	Length, m	Thickness, m	Height, m	Inertia, kg m^2
Shoulder–elbow		0.73[a]			
Elbow–tip					
RF		0.96[a]			
FF		0.71[a]			
Beam element					
Link 1	0.11	0.51	0.0016	0.05	
Link 2					
RF	0.16	0.76	0.0016	0.05	
FF	0.11	0.51	0.0016	0.05	
Joints					
Shoulder rotor	2.5				1.1
Elbow	6				0.47
Payload	0.55				0.0001

[a]Overall length.

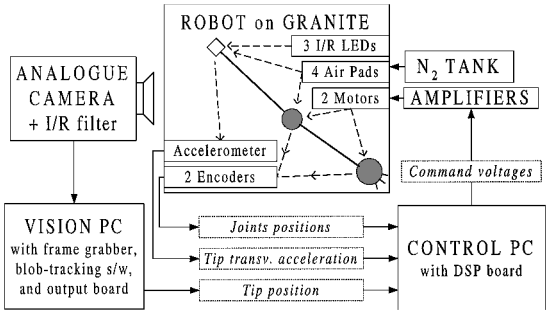

Fig. 4 Block diagram of the SRS testbed.

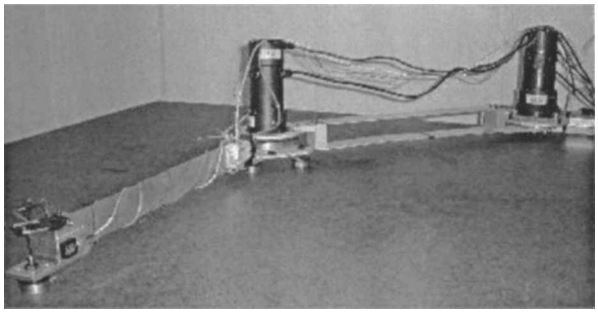

Fig. 5 SRS robot in RF configuration, with rigid first link and flexible second link; shoulder joint at the top-right corner.

The granite table supports the overall manipulator and constitutes the work plane. It has dimensions $1.8 \times 2.4 \times 0.3$ m. The stone surface is smoothed with an overall accuracy of $\pm 10^{-6}$ m.

The manipulator is a planar two rotational DOF system, whose base, that is, the stator of the shoulder joint, is rigidly connected to one side of the granite table. The robot model has a modular design: Both links can be either rigid or flexible, as regards the bending on a plane parallel to the granite table surface. A rigid link is constituted by two beam elements, having rectangular section, screwed to the contour joints with the wider side parallel to the granite table. A flexible link is constituted by only one beam element mounted with the wider side perpendicular to the table. All of the structural elements of the robot are made of aluminum alloy 6061. For the experiments reported in this paper, the manipulator was used in the following two configurations, whose geometric characteristics are reported in Table 1.

1) The manipulator with a rigid first link and flexible second link (RF) is shown in Fig. 5. The first two bending frequencies of the second flexible link, experimentally determined, are at 0.58 and 8.5 Hz.

2) The second configuration is a manipulator with both links flexible (FF). In this case, the vibration modes are functions of the position of the second link with respect to the first. It was chosen to consider the modes with the manipulator in a completely extended configuration, that is, with the second link parallel to the first, because that was the configuration at the middle of the considered reference maneuver. The first two elastic modes for this configuration are at 0.22 and 1.2 Hz.

Table 2 Main data of the SRS motors

Property	Shoulder motor	Elbow motor
Type	HD RFS-25/6018	HD RFS-20/6012
Maximum output torque, N · m	100	57
Torque constant, N · m · A^{-1}	11.0	10.2
Mass, kg	6.4	4.2
Gear ratio	50	50

The robot is supported on the granite table by four air pads, three of them mounted at the elbow and one at the payload. The friction is practically null between the table and the pads, and a very good approximation of the microgravity condition is obtained as regards the motion on the plane. The air pads are fed by compressed nitrogen at 3×10^5 N/m^{-2}.

A personal computer Pentium III/500 MHz, hosting a Motorola DS-1103 PPC controller board, is used for the real-time control. The control algorithm, developed in MATLAB®-Simulink, is compiled and downloaded to the PPC board using Dspace system. The sample rate was set at 1 kHz for all of the experiments.

For the actuators, two dc brushed motors with harmonic drive gearing are mounted on the SRS. The motors' data are reported in Table 2: In particular, the torque constants were experimentally determined by using the method proposed in Ref. 19. Because the actuators are highly overdimensioned with respect to the dimensions of the links, the joint torsion is negligible. Each motor is powered by a Kepco BOP 72-3M amplifier, driven by the command signal of the control system.

The following sensors have been used.

Two optical incremental encoders with a resolution at output of 18,000 pulses/round are directly mounted onto the two motors' shafts, to measure the angular displacement. The angular speed measurement is obtained online by backward difference from the encoders' angular measurement, with a second-order low-pass digital filter having cut-off frequency at 50 Hz.

An optical position sensor was used, which is able to measure the position of the tip of the robot on the motion plane, with a frequency of 60 Hz. A 640×480 pixel, PULNIX TM-6701 monochrome camera with infrared filter is mounted at an height of 2.1 m above the granite table. The output from the camera is sent to a CORECO frame grabber card, hosted by a personal computer Pentium III/600 MHz. A blob-tracking software, by Agris-Schoen Vision Systems, analyzes the data from the camera, and sends to the Dspace system with two signals proportional to the Cartesian coordinates of the tracked point. That point is one of three infrared light emitter diodes, disposed at the vertexes of a right triangle, mounted at the manipulator tip. The signals from the optical sensor were filtered online by a first-order low-pass analog filter at 20 Hz and offline with an eighth-order Butterworth low-pass digital filter at 5 Hz. The optical position sensor had resolution of $\sim$1 mm and accuracy of $\sim$1 cm. The relatively low accuracy, between the position measured by the optical system and the actual position on the granite table, was mainly due to uncompensated optical effects, calibration imprecision, and noise in the acquisition chain.

To have a measure of the tip oscillation independent of the optical system, a Kistler K-beam 8304B accelerometer is used to measure the absolute acceleration, in the direction transversal to the second link at the tip of the manipulator. The resolution is 10^{-4} g, and the range ± 2 g.

V. Experimental Results

In this section, the most significant experiments of preshaped input tracking control, carried out on the SRS testbed, are described, and their results are analyzed. Reference 20 has a complete report of the series of experimental tests.

The links of the manipulator are treated as if they were rigid, to compute, offline before the experiments, the feedforward command

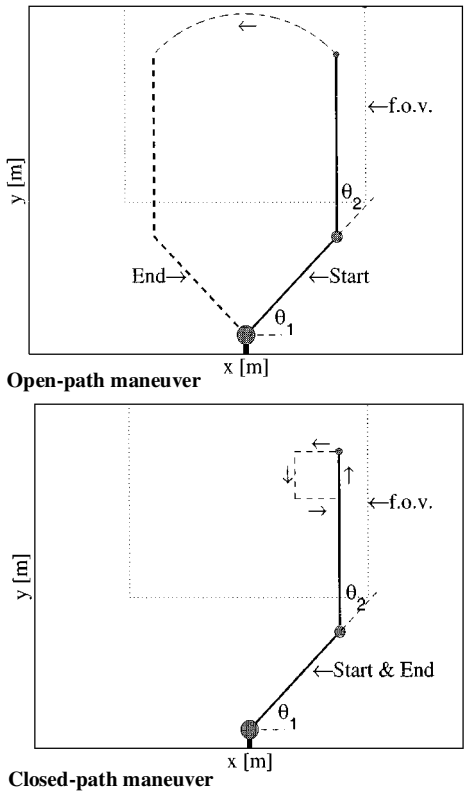

Fig. 6 Two considered reference maneuvers on the granite table surface (dotted rectangular shape is camera's field of view).

torques used by the sliding-mode control to follow the reference joints motion.

The following paragraphs describe the reference maneuvers (shown in Fig. 6) that have been considered.

During the open-path maneuver, the joints of the manipulator slew in opposite directions from rest to rest, over an angle of $\pi/2$. In particular, θ_1 goes from $\pi/4$ to $3/4\pi$ and θ_2 from $\pi/4$ to $-\pi/4$. This maneuver was directly designed in the joint space to avoid any problem due to singularity of the kinematic inversion. The feedforward torques are derived via dynamic inversion, from the reference angular accelerations, speeds, and positions, assuming a two-link manipulator rigid model. The equations of motion of that model have the form of Eq. (5). In particular, the joints friction and the gravitational terms are considered zero; the complete expression of the inertia matrix and of the matrix of Coriolis and centrifugal terms is reported in Ref. 20 and reflects the data of the experimental manipulator SRS reported in Table 1.

The following four types of reference angular accelerations (RA) have been tested along the open-path maneuver. Figure 7 shows the shoulder joint acceleration profiles. Because of the symmetry of the maneuver, the profiles for the elbow joint are the same, changed in sign. For the FF configuration, only the input shaped profiles change because of the different vibration frequencies.

1) The minimum travel time for RA_1, bang–bang, was taken as 4.5 s for each joint, and the maximum angular acceleration was, consequently, 0.31 ms^{-2}, computed using Eq. (4), with $\alpha = 0$.

2) We used the following ZVD input shaper, with impulses calculated as in Fig. 1, considering the system undamped for RA_2, input shaping applied to the bang–bang profile:

$$\begin{bmatrix} t_i \\ A_i \end{bmatrix} = \begin{bmatrix} t_0 & (t_0 + T/2) & (t_0 + T) \\ 0.25 & 0.5 & 0.25 \end{bmatrix}$$

where T is the period of the vibration to be suppressed. That is, 1.72 s for the RF configuration and 4.54 s for the FF configuration. The convolution is achieved, in practice, by superimposing three shifted copies of the original signal, scaled by the value of the pulses' amplitude.

Table 3 Values of the controller's parameters used for the experiments

Parameter	Value
K	$\begin{bmatrix} 10 & 0 \\ 0 & 10 \end{bmatrix}$
Λ	$\begin{bmatrix} 30 & 0 \\ 0 & 15 \end{bmatrix}$
a	20
b	1
$k_1\|\tilde{M}\|$	2
$k_2\|\tilde{C}\|$	2
$k_3\|\tilde{g}\|$	0
f_s	5.6
f_d	0.2

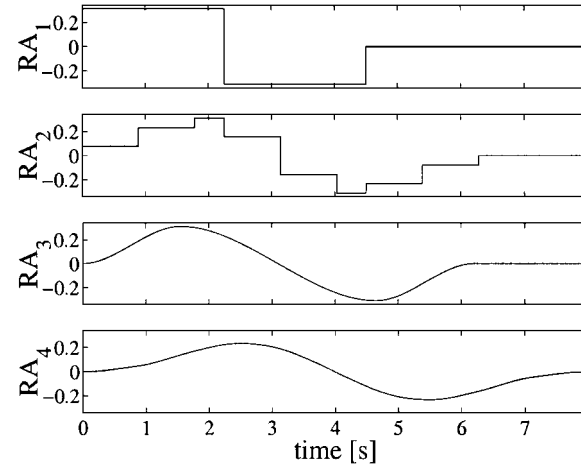

Fig. 7 Four angular acceleration profiles, in rad/s^2, tested on the open-path maneuver, for the shoulder joint and RF configuration.

3) The maximum value of the smoothing parameter has been considered ($\alpha = 0.25$), and the joint angular accelerations obtained by Eqs. (2) for RA_3, smoothed bang–bang.

4) Again the three-impulses input shaper has been applied for RA_4, input shaping applied to the smoothed bang–bang profile.

For the closed-path maneuver, a square path was considered, with a side of 0.25 m. This kind of maneuver is challenging because the change in the commanded direction at the corners of the square is likely to induce vibrations. The starting configuration of the manipulator is equal to the open-maneuver case. In this case, the maneuver was designed in the task space; kinematic inversion was carried out taking as reference a trajectory without singularity and considering the manipulator as if it was rigid. Then the reference command torques were derived via dynamic inversion as for the preceding case. The manipulator is at rest at each corner of the reference square path, and along each side of the square follows one of the two following reference accelerations.

1) For bang–bang acceleration, the minimum travel time along each side of the square was taken as 1 s, and the reference acceleration, speed, and position on the path were computed consequently.

2) Unlike for the open maneuver, for input shaped bang–bang reference acceleration along each side of the square, the convolution is applied to the acceleration along the path.

Preliminary tests were executed to set the values of the sliding-mode controller parameters: The chosen values are reported in Table 3. Then the controller was used to track the two reference maneuvers already described, following the different angular acceleration profiles.

All of the experiments reported in this paper were carried out several times, with a very good repeatability of the results.

A. Experiments on Tracking the Open-Path Maneuver

Table 4 reports the most significant data regarding the experiments of tracking of the open-path maneuver by the robot in the two

configurations RF and FF, with the four described RAs. The amplitude of residual oscillation was computed considering the measure either from the camera or from the accelerometer.

The application of input shaping reduces the residual vibration of about 87% with respect to the bang–bang acceleration, in the case with only the second link flexible, and of about 98% in the case with both links flexible. These results demonstrate clearly the effectiveness of the input shaping approach.

Table 4 Main data of the experiments of tracking of the slewing maneuver, with the SRS manipulator in RF and FF configurations

	RF		FF	
RA	t_f,[a] s	R,[b] mm	t_f,[a] s	R,[b] mm
Bang–bang (RA_1)	4.50	55	4.50	700
↪ Input shaped (RA_2)	6.28	7.5	9.04	15
Smoothed (RA_3)	6.20	6.5	6.20	625
↪ Input shaped (RA_4)	7.98	3.5	10.74	10

[a]Maneuver time. [b]Amplitude of the residual vibration at the tip.

Remarkably, although in the case of the configuration with one flexible link the smoothing works about the same as the input shaping, in the case when both the links are flexible, only the input shaping approach is effective in reducing the vibration to a reasonable value. This interesting result is probably because, when the vibration period becomes of the same order of the bang–bang command period, the smoothed command effectiveness decreases. One possible interpretation is that the smoothed bang–bang commands are very similar to bang–bang functions that have been subjected to a low-pass filter. Therefore, their performance varies considerably with the system parameters and, in particular, its modes. However, the input shaping commands are bang–bang functions that have been subjected to a notch filter that targets the frequencies in the system. In this way, the input shaping is more intelligent than the smoothed profile, and its performance is not so highly dependent on the variations of the system parameters.

Figures 8 and 9 show the detailed results of the first two tests of Table 4. The tracking of the joint angles during the trajectory was very good in all cases. The reference and actual curves are laid one on the other in Figs. 8a, and the tracking of the angular speed

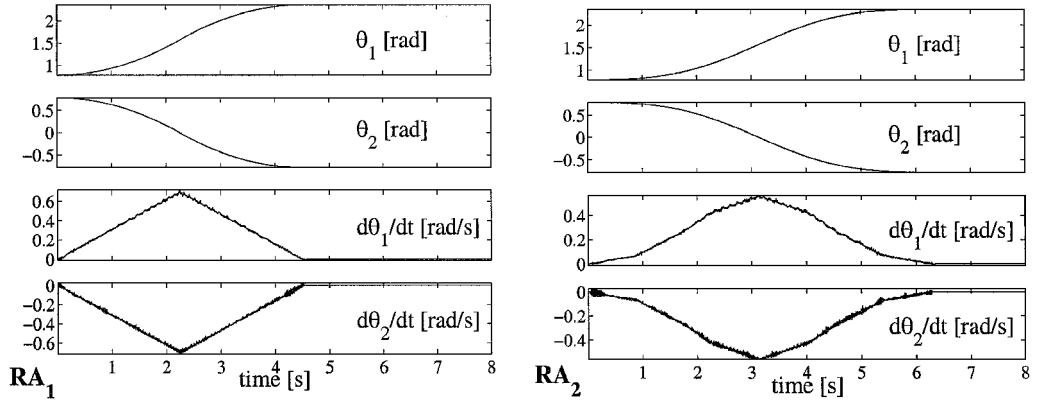

a) Angular positions and speeds, measured and reference (····)

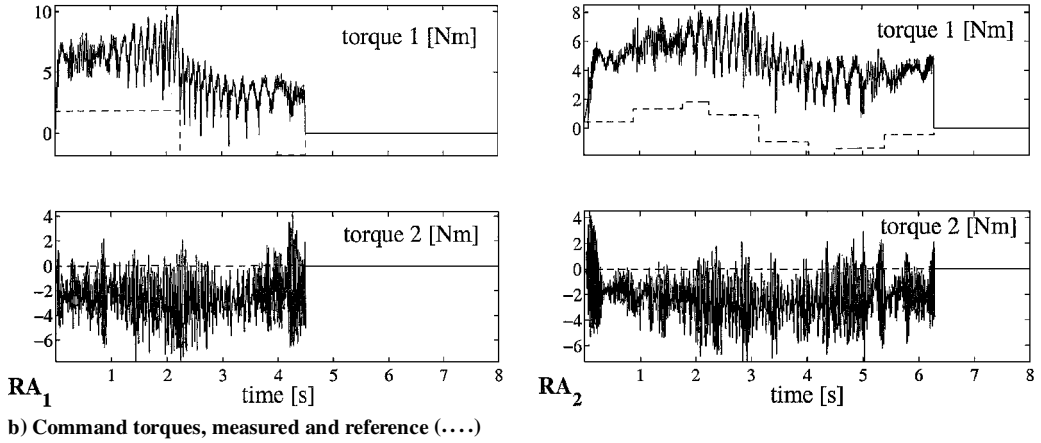

b) Command torques, measured and reference (····)

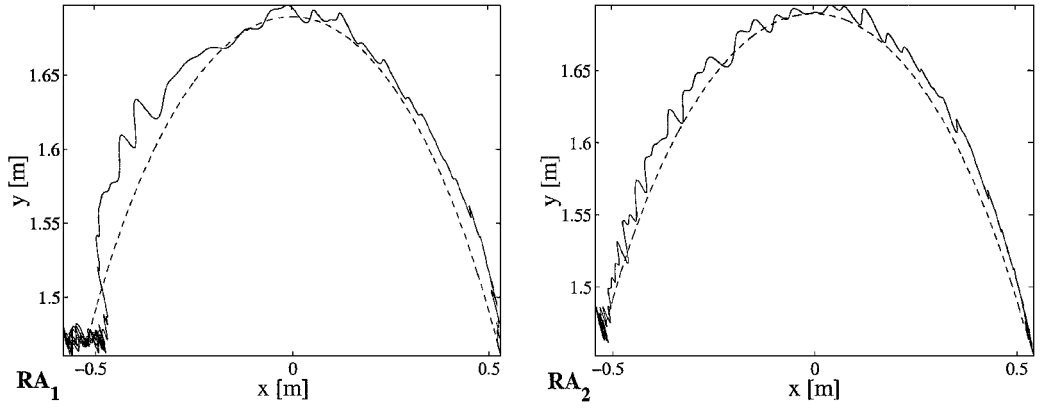

c) Path of the robot tip, measured and reference (····)

Fig. 8 Detailed results of two experiments, carried out with the robot in RF configuration; left column case of bang–bang RA_1 and right column case of input shaped bang-bang acceleration RA_2.

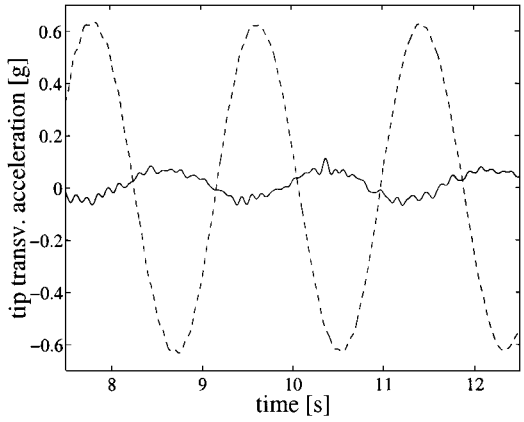

Fig. 9 Residual transversal accelerations at tip for RF configuration RA_1, ····, and RA_2.

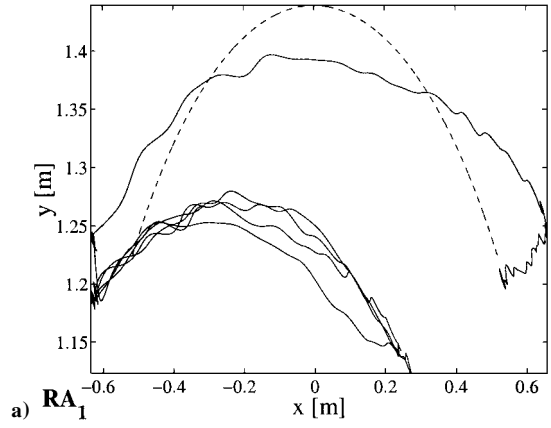

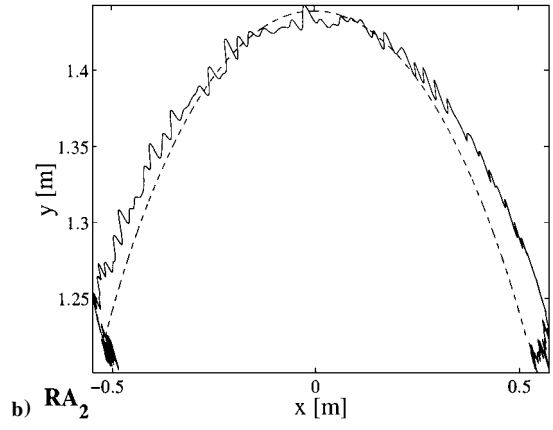

Fig. 10 Path of robot tip on the workspace, reference (····) and actual, for two tests with FF configuration case.

was also acceptably good. The orders of magnitude of the errors were 10^{-3} rad for the angles and 10^{-2} rad/s for the angular speeds. This fact proves the effectiveness of the sliding-mode tracking controller. Figures 8b, showing the command torques, show clearly the important contribution of the friction compensation in the maneuver tracking. Because of the high stiction of the joints, the feed-forward commands alone are not able to move the joints from their initial position. Figures 8c, showing the robot tip path, clearly show the effect of input shaping. That effect is evident, also during the motion, especially in the reduction of the overshooting. The reference line in Figs. 8c is calculated from the reference joint displacements, with a direct kinematic transformation. The rather low accuracy of the camera sensor does not affect our conclusions, based on comparisons of the sensor's outputs and confirmed by the measure of the accelerometer.

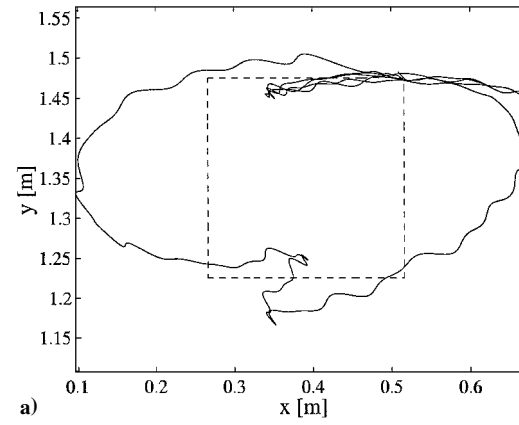

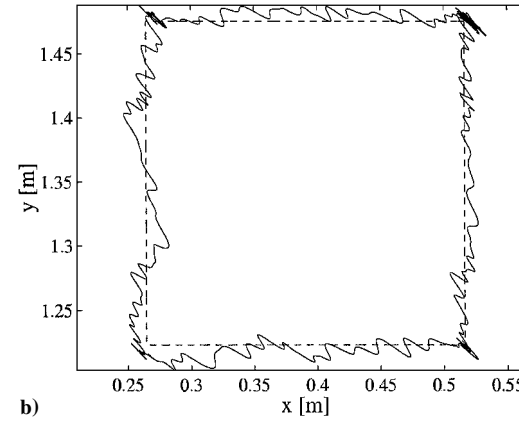

Fig. 11 End-point trajectory measured by the optical sensor and reference (····): a) closed path maneuver with bang–bang joints acceleration and b) same reference maneuver but with input shaped bang–bang joints acceleration.

A second proof of the effect of input shaping is given in Fig. 9, where the residual tip transversal acceleration is reported. The improved performance is really evident.

As regards the experiments of the robot with both flexible links, the very good performance of input shaping with respect to the bang–bang and smoothed bang–bang case, already shown in Table 4, is immediately evident from Fig. 10. In the bang–bang case, the robot tip goes out of the camera's field of view during the residual oscillation. The tip motion in the smoothed bang–bang case is similar to the bang–bang case.

B. Experiments on Tracking the Closed-Path Maneuver

Bang–bang and input-shaped bang–bang reference acceleration along each side of the square have been tested on the robot in the RF configuration, that is with rigid first link and flexible second link.

As shown in Fig. 11, the input shaping is clearly effective in reducing the vibration, also along the closed-path maneuver. Whereas with the bang–bang acceleration profile along each side the maximum tracking error is ∼15 cm, input shaping reduces it to ∼2 cm.

These experimental results are in good agreement with the results reported in Refs. 5 and 11.

VI. Conclusions

A series of experimental tests on the tracking control of a very flexible planar robot, floating on air pads on a granite table testbed, has been carried out. Two configurations of the robot were tested: 1) with first link rigid and second flexible and 2) with both links flexible.

The effectiveness of the input shaping method has been clearly demonstrated in reducing the vibrations of the links during near-minimum-time maneuvers, either open or closed, for both robot configurations.

A comparison of the input shaping approach with a second command shaping technique, which consists in smoothing the

bang–bang reference signal, was carried out and led to the following interesting result: Whereas the smoothing approach is as effective as input shaping in the case of only one flexible link, in the case of both links flexible, only the input shaping approach is effective. That is probably because, when the vibration period becomes of the same order as the bang-bang command period, the smoothed command effectiveness decreases. The change of the smoothing parameters α does not affect that result. On the contrary, input shaping, either applied to the bang–bang reference acceleration or to the smoothed bang–bang, still improves the performance.

A recently introduced sliding-mode tracking control method, with friction compensation, has been applied for the first time in our experiments to follow the reference commands. Very good performance in tracking the joint motion has been achieved, despite the high and poor modeled stick–slip friction of the harmonic drive geared motors powering the robot. The tracking precision could be probably still improved using tachometer sensors in addition to the encoders.

In conclusion, the utilization of input shaping, associated to a sliding-mode tracking control was found to solve the problem of tracking a reference maneuver with a flexible links manipulator. This is a promising technique and, in principle, it could be directly applied to the existing space manipulators. In fact, only the actuators and sensors naturally present at the manipulator joints are used. The computation requirements are relatively low, and the method can be applied to track any reference maneuver.

Acknowledgments

The authors wish to thank Hong-Jen Chen for his useful advice in the design of the real-time controller software and Gangbing Song and Arun Banerjee for the interesting discussions on the research topics. Moreover, we would like to thank the anonymous reviewers for their helpful comments.

References

[1]Smith, O., *Feedback Control Systems*, McGraw–Hill, New York, 1958, pp. 331–345.

[2]Singer, N., and Seering, W., "Preshaping Command Inputs to Reduce System Vibration," *Journal of Dynamic Systems, Measurement, and Control*, Vol. 112, No. 3, 1990, pp. 76–82.

[3]Singhose, W., Banerjee, A., and Seering, W., "Slewing Flexible Spacecraft with Deflection-Limiting Input Shaping," *Journal of Guidance, Control, and Dynamics*, Vol. 20, No. 2, 1997, pp. 291–298.

[4]Banerjee, A., and Singhose, W., "Command Shaping for Nonlinear Tracking Control of a Two-Link Flexible Manipulator," AAS/AIAA Astrodynamics Specialists Conf., American Astronautical Society, AAS Paper 97-121, Aug. 1997.

[5]Banerjee, A., and Singhose, W., "Command Shaping in Tracking Control of a Two-Link Flexible Robot," *Journal of Guidance, Control, and Dynamics*, Vol. 21, No. 6, 1998, pp. 1012–1015.

[6]Song, G., Buck, N., and Agrawal, B., "Spacecraft Vibration Reduction Using Pulse-Width Pulse-Frequency Modulated Input Shaper," *Journal of Guidance, Control, and Dynamics*, Vol. 22, No. 3, 1999, pp. 433–440.

[7]Junkins, J., Rahman, Z., and Bang, H., "Near Minimum-Time Maneuvers of Distributed Parameter Systems: Analytical and Experimental Results," *Journal of Guidance, Control, and Dynamics*, Vol. 14, No. 2, 1991, pp. 406–415.

[8]Hecht, N., and Junkins, J., "Near-Minimum-Time Control of a Flexible Manipulator," *Journal of Guidance, Control, and Dynamics*, Vol. 15, No. 2, 1992, pp. 477–481.

[9]Mimmi, G., Pennacchi, P., and Bernelli-Zazzera, F., "Minimizing Residual Vibration for Flexible Manipulator in Point to Point Operations," *Applied Mechanics in the Americas*, Vol. 8, 1999, pp. 1565–1570.

[10]Tuttle, T. D., and Seering, W. P., "Experimental Verification of Vibration Reduction in Flexible Spacecraft Using Input Shaping," *Journal of Guidance, Control, and Dynamics*, Vol. 20, No. 4, 1997, pp. 658–664.

[11]Singhose, W., and Singer, N., "Effects of Input Shaping on Two-Dimensional Trajectory Following," *IEEE Transactions on Robotics and Automation*, Vol. 12, No. 6, 1996, pp. 881–887.

[12]Magee, D., and Book, W., "Optimal Filtering to Minimize the Elastic Behavior in Serial Link Manipulators," *American Control Conference*, Inst. of Electrical and Electronics Engineers, New York, Vol. 8, 1998, pp. 2637–2642.

[13]Hillsley, K., and Yurkovich, S., "Vibration Control of a Two-Link Flexible Robot Arm," *IEEE International Conference on Robotics and Automation*, Vol. 4, Inst. of Electrical and Electronics Engineers, New York, 1991, pp. 2121–2126.

[14]Drapeau, V., and Wang, D., "Verification of a Closed-Loop Shaped-Input Controller for a Five-Bar-Linkage Manipulator," *IEEE International Conference on Robotics and Automation*, Vol. 3, Inst. of Electrical and Electronics Engineers, New York, 1993, pp. 216–221.

[15]Armstrong-Helouvry, B., Dupont, P., and de Wit, C. C., "A Survey of Models, Analysis Tools and Compensation Methods for the Control of Machines with Friction," *Automatica*, Vol. 30, No. 7, 1994, pp. 1083–1138.

[16]Song, G., "Robust Control and Adaptive Robust Control of Robot Manipulators," Ph.D. Dissertation, Columbia Univ., New York, 1995.

[17]Shiller, Z., and Dubowsky, S., "Robot Path Planning with Obstacles, Actuator, Gripper, and Payload Constraints," *International Journal of Robotics Research*, Vol. 8, No. 6, 1989, pp. 3–18.

[18]Romano, M., "Tracking Control of Flexible Space Manipulators: Simulations and Experiments," Ph.D. Dissertation, Politecnico di Milano, Milan, Italy, Dec. 2000.

[19]Corke, P., "In Situ Measurement of Robot Motor Electrical Constants," *Robotica*, Vol. 14, No. 4, 1996, pp. 433–436.

[20]Romano, M., "Experiments on Near-Minimum-Time Control of a Flexible Space Robot Using Command Shaping Techniques and Joint Friction Compensation," Spacecraft Research and Design Center, Research Rept. SRDC-00-1, Naval Postgraduate School, Monterey, CA, 2000.